AD-A155 581 FINITE-DIFFERENCE COMPUTATIONS OF ROTOR LOADS(U) ARMY 1/1
AVIATION SYSTEMS COMMAND ST LOUIS MO
F X CARADONNA ET AL. APR 85 USAAVSCOM-TR-85-A-3
UNCLASSIFIED NASA-TM-86682 F/G 12/1 NL

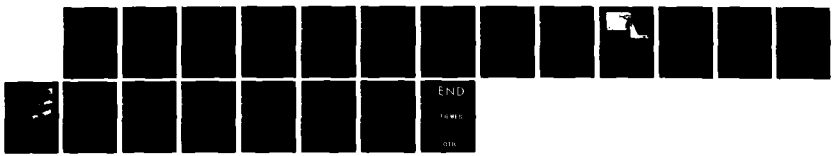

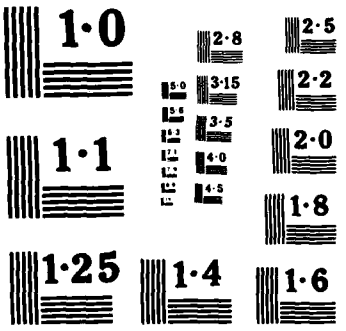

NASA Technical Memorandum 86682

USAAVSCOM Technical Report 85-A-3

Finite-Difference Computations of Rotor Loads

F.X. Caradonna and C. Tung

April 1985

National Aeronautics and Space Administration

United States Army Aviation Systems Command

85 6 4 037

NASA Technical Memorandum 86682

USAAVSCOM Technical Report 85-A-3

Finite-Difference Computations of Rotor Loads

F. X. Caradonna

C. Tung, Aeromechanics Laboratory, U. S. Army Research and Technology Laboratories (AVSCOM)
Ames Research Center, Moffett Field, California

April 1985

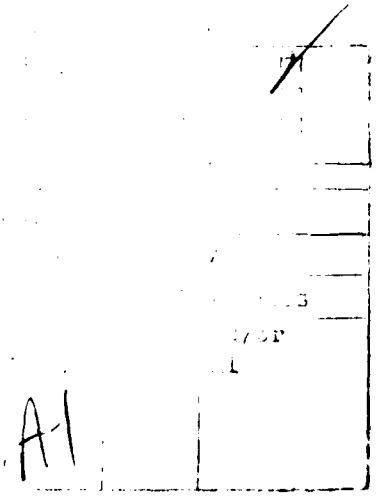

National Aeronautics and
Space Administration

Ames Research Center
Moffett Field, California 94035

United States Army
Aviation Systems
Command
St. Louis, Missouri 63120

FINITE-DIFFERENCE COMPUTATIONS OF ROTOR LOADS

F. X. Caradonna and C. Tung
Aeromechanics Laboratory, U.S. Army Research and Technology Laboratories--AVSCOM
NASA Ames Research Center
Moffett Field, California

Abstract

This paper demonstrates the current and future potential of finite-difference methods for solving real rotor problems which now rely largely on empiricism. The demonstration consists of a simple means of combining existing finite-difference, integral, and comprehensive loads codes to predict real transonic rotor flows. These computations are performed for hover and high-advance-ratio flight. Comparisons are made with experimental pressure data.

Notation

$A = M_T^2/AR^2\delta^{2/3}$

AR = R/c, aspect ratio

$B = 2M_T^2 f/AR\delta^{2/3}$

$C = 1/AR^2\delta^{2/3}$

C_L = lift coefficient

C_T = thrust coefficient

c = chord

D = Bg

$F = \frac{1 - f^2M_T^2}{\delta^{2/3}}\Phi_x - M_T^2\frac{\gamma+1}{2}f\Phi_x\Phi_x$

$f = y + \mu \sin\psi$

$g = x/AR - \mu\cos\psi$

M_T = tip Mach number

R = blade radius

r = radial station

x = x'/c, nondimensional streamwise coordinate (prime denotes a physical quantity)

y = y'/R, nondimensional spanwise coordinate (prime denotes a physical quantity)

$z = z'/c\delta^{1/3}$, scaled nondimensional normal coordinate (prime denotes a physical quantity)

α = angle of attack, deg

α_p = partial angle of attack, deg

γ = specific heat ratio

δ = thickness ratio

θ_c = collective pitch angle, deg

θ_{1c} = longitudinal cyclic input, deg

θ_{1s} = lateral cyclic input, deg

μ = advance ratio

$\Phi = \phi'/\Omega Rc\delta^{2/3}$, a scaled velocity perturbation potential

Φ_n = normal derivative of Φ

Φ_{nn} = second normal derivative of Φ

ψ = azimuthal angle, deg

Ω = angular speed

σ = solidity

Introduction

The design of new rotor systems can be a risky undertaking. Therefore, most of these machines are derivatives or scaled versions of other well-proved rotor systems. Much of the risk of helicopter development stems from an inadequate understanding of and ability to predict the performance-defining physical behavior of the rotor--especially the aerodynamic behavior. Most of the various flow phenomena that limit or define the

Presented at the International Conference on Rotorcraft Basic Research, National Institute of Environmental Health Sciences, Research Triangle Park, North Carolina, February 19-21, 1985.

capabilities of a helicopter (e.g., wake formation, dynamic stall, acoustic propagation, transonic behavior, blade/wake interactions, and other unsteady loading and drag sources) are problems the understanding of which has not progressed far beyond the empirical level. The translation of our empirical understanding into a more reliable predictive ability probably awaits the development of more comprehensive numerical modeling techniques than currently exist. At present, our best computational schemes are built around various integral methods, of which lifting-line theory is the most commonly used. These methods are, in the main, limited to the prediction of linear compressible flows. The use of tabular airfoil data extends the validity of these methods, but only to the extent that two-dimensional, steady flow is representative of the rotor flow.

A much more general predictive tool is to be found in the differential methods of flow modeling. This class of schemes (which includes the finite-difference methods) requires a high investment in computer capability but has no intrinsic physical modeling limitations. Finite-difference methods for the solution of various high-speed and high-lift problems are becoming commonplace in fixed-wing aircraft design. However, such methods have not yet been employed for rotary-wing work because of the greater flow complexity. The intent of this paper is to demonstrate a means whereby existing codes (both integral and differential) may be combined to solve realistic rotor flow problems, which have heretofore been treated empirically.

Choice of Flow Models for Various Flow Problems

The helicopter's various flow problems can require a wide number of models. If one were to compute an entire vehicle with accurate modeling of all relevant phenomena nothing less than a massive Navier-Stokes (NS) solver would be required. But far more modest goals have confounded us for years. The oldest of these is the rotor free-wake problem. All integral (vortex lattice, etc.) methods have failed to produce a reliably workable tool--and for unknown reasons. A few preliminary finite-difference attacks[1,2] on the problem have not done better, but this work is only in its infancy. The best current approaches are still those that use prescribed wake models. Retreating-blade stall is another problem that is best handled empirically. The problem has been treated with NS codes, but these are not yet satisfactory because of inadequate turbulence modeling. One area which seems no longer to be beyond our grasp is the high-speed, advancing-blade problem. Separation does not usually occur here, and the essential physics is inviscid. Euler codes are appropriate for these flows, but may only be required when shocks occur that generate appreciable vorticity. Flows with weaker shocks are much more efficiently treated by potential methods. Even with this simplest of finite-difference models, it is not currently feasible to treat an entire rotor flow, and the problem becomes one of efficiently embedding a local finite-difference solution in a global solution obtained by other means (probably an integral method). Such a scheme will still be nonlinear, three dimensional, and unsteady and could greatly reduce or eliminate the need for airfoil tables.

Potential Equations of Motion and Boundary Conditions

The starting point for the various potential formulations is the mass conservation and Bernoulli's equation, together with the assumption of irrotationality. This system of equations will conserve mass, energy, and entropy when solved in a divergence form[3] that maintains the separate identities of density and potential. However, a number of significant nonconservative[4] methods solve only for potential. Such schemes would only be conservative if combined with a shock-fitting scheme. (Note that conservation implies the ability to accurately predict shock motion and the resulting load variations.) The simplest potential equations involve various small-perturbation approximations. This class of equations all have the form

$$A\Phi_{\psi\psi} + B\Phi_{x\psi} = F_x + \Phi_{zz} + C\Phi_{yy} + D\Phi_{xy} \qquad (1)$$

where F is a nonlinear flux term that is a function of Φ_x. This equation is derived by means of a small cross-flow assumption and only one nonlinear term (that contained in F) is retained. A fortunate consequence of the small-perturbation approximation is that the equation remains conservative in spite of its not explicitly involving density.

The boundary conditions for Eq. (1) are shown in Fig. 1. The computation region shown is a box which contains the outer section of a rotor. The boundary conditions on the faces of this box are usually undisturbed flow conditions, except for the inboard face where two-dimensional flow is assumed. The surface tangency condition is expressed by specifying the surface slopes on a mean plane of the rotor. In order to represent vortices and vorticity sheets, interior planes of potential discontinuity are imposed. In Fig. 1, two such planes are shown. One plane, which is aft of the trailing edge, models the trailing and shed vorticity. Another sheet below the rotor models a vortex located at the edge of this sheet.

The model shown in Fig. 1 automatically takes account of the inflow produced by the vorticity in the computation region. However, the vorticity in the remainder of the total rotor flow field is not automatically accounted for. The simplest way to include this outer flow seems to be to compute a partial angle of attack, α_p, which is a result of the vorticity in the outer region, and impose it on the mean surface boundary condition. In return, the loads computed by the finite-difference computation provide the basic vorticity distribution for the outer flow computation. This exchange of flow angle and load information between the inner and outer flow regions is the heart of a finite-difference embedding scheme. This embedding will now be demonstrated for two different flight situations.

Model Hover Testing

The simplest problem that requires the above embedding procedure is a high-speed hover.[5,6] This problem is relatively simple because it is steady, and the required validation data are fairly easy to obtain on the model scale. Figure 2 shows a 7.5-ft-diam model which was tested in the Aeromechanics hover facility. The model was equipped with a hub-mounted Scanivalve assembly which permitted the measurement of pressure at 120 points on the rotor. Since the wake geometry is unpredictable, its measurement is a vital element of such testing. These measurements were performed with traversing hot wires. The resulting information was then used as the required prescribed wake data in an integral flow code--in this case the Analytic Method, Inc. code, HOVER.[7] For subcritical tip speeds, HOVER predicts the measured lift distribution very well. However, for supercritical tip speeds, HOVER cannot treat the resulting transonic nonlinearity, and it becomes necessary to use an embedded finite-difference solution. For the present problem a steady rotor, small-perturbation code was used.[8] The boundary conditions employed were the same as depicted in Fig. 1, except that two vortices were included in the computation region. In the course of the computation, the locations of the vortices were fixed by the experimental data, and their strength was equated to the maximum blade bound circulation. A typical comparison of measured and computed pressure distribution is shown in Fig. 3 for a tip speed $M_T = 0.877$.

The fact that the finite-difference embedded solution reproduces the measured loads well beyond the range of validity of the linear HOVER code demonstrates the validity of the small-perturbation method. It also shows that the scheme keeps consistent account of vorticity, in spite of this vorticity being split into two entirely separate codes.

Forward Flight Computations

Transonic flows are intrinsically unsteady, and advancing-blade transonic flows can be among the most unsteady flows of all. Nevertheless, tabular profile data take no account of this unsteadiness. Such flows are difficult to compute if the wake is to be accounted for, as was done in the previous hover case. For such cases, the vortices from previous blades are no longer neatly aligned with a coordinate; instead, they assume a wide range of orientations as they move through the grid. At present, such computations are being attempted only in two dimensions. However, a simple first approach to the problem is to account for the inflow entirely with a partial angle of attack, with no vortex in the grid other than the trailing and shed vorticity sheet. Such a scheme is almost certainly valid at high advance ratios where the induced inflow is small. This scheme has been implemented in a code[9] we call FDR (Finite-Difference Rotor Code); FDR solves the low-frequency variant of Eq. (1) (that is, $A = 0$).

Another problem with forward flight computations is that the blade is constantly responding to the varying loads, and a trim solution must be obtained. The problem here is one of efficiency. Trim solutions are iterative processes often requiring the rough equivalent of computing 10 rotor revolutions. This much computing is no problem when the blade forces are obtained from a table, but it would be prohibitive for a finite-difference solution. A solution to this problem is to perform the basic finite-difference solution outside the central trim iteration.[10] Inside the trip loop, tables (or any fast, convenient approximate to a finite-difference solution) can be used to find a load correction based on the new blade motion. That is,

$$C_L(\alpha) = C_{L_{FD}}(\alpha_{old}) + C_{L_{table}}(\alpha) - C_{L_{table}}(\alpha_{old})$$

where α and α_{old} are the angles of attack from the current and previous trim loops, respectively. The solution is converged when $\alpha \to \alpha_{old}$ and the lift correction vanishes; that is, when the finite-difference lift is fully consistent with the rotor inflow and motion. This process has been followed using the comprehensive rotor code CAMRAD[11] to provide the outer inflow, blade motion, and trim computations.

The matching of the CAMRAD and FDR codes is summarized in the flow diagram shown in Fig. 4. The process is started by obtaining a trimmed,

nonuniform inflow solution with the lift totally obtained from airfoil tables. This is, in fact, the normal operation of CAMRAD, except that partial wake-influence coefficients are computed in addition to the usual full-wake values. These partial coefficients are used to obtain partial angles of attack, which in turn are fed to the FDR. The lift distributions so obtained are then fed to the CAMRAD trim loop where the airfoil tables are used to find a lift correction. The process now iterates between the FDR and the trim loop until convergence of α is achieved. This scheme is an efficient one because it keeps all the time-consuming computations (the influence-coefficient and especially the finite-difference calculations) out of the innermost trim loop. It has been our experience to date that the convergence of this scheme is extremely rapid.

A suitable body of experimental data on which to test the present code was obtained at a recent model-rotor test performed at the Deutsch-Niederlaendischer Windkanal (DNW).[12] The rotor is a 1/7-scale model of the Cobra operational load survey (OLS) blades (Fig. 5). Like the OLS blades, the model is pressure instrumented (but not nearly so densely). At the present time, a small amount of the pressure data is available. Moreover, the model is fairly uncomplicated and is a good first test case for the present method. The rotor is a teetering rectangular blade with a linear twist and has a modified BHC-540 airfoil. Since the model is quite stiff, we have not considered blade bending or twisting in the present computations.

The available data sets are high-speed cases. A typical run, which we have computed, has a tip Mach number M_T of 0.663, an advance ratio μ of 0.298, and a $C_T/\sigma = 0.0769$. For this case, the contribution of the grid-enclosed trailing vortex to the full angle of attack is seen in the spanwise distributions of α and α_p at $\psi = 90°$ (Fig. 6). At this azimuth, a tip vortex passes beneath the rotor at 0.7R. Accordingly, α is augmented outboard and diminished inboard of this location. Since the rotor lift varies similarly, the trailing vorticity will have an opposing effect on the induced flow of the vortex. Removing this opposing effect results in an α_p distribution with a much stronger variation. This large difference between α and α_p demonstrates the importance of keeping a consistent account of the wake with a matched scheme. In Fig. 6, the distribution of α, α_p, $C_{L_{FD}}$ (lift computed in FDR), and C_L (the lift computed in the CAMRAD trim loop) are shown for three iterations. The $N = 0$ iteration is the starting CAMRAD lifting-line solution. All subsequent iterations are complete integral-differential cycles. For $N = 1$ there is a moderate difference between the $C_{L_{FD}}$ and the C_L. However, for $N = 2$ there is no difference between them, and the solution appears completely converged. Another view of the convergence is shown in Fig. 7, which shows the azimuthal variation of α for various iterations. Again the solution appears completely converged by the second iteration, with the greatest change occurring in the second quadrant.

Figure 8 shows the spanwise variations of C_L for a wide range of azimuths for the pure CAMRAD and the converged CAMRAD-FDR solutions. It is seen here that the effect of switching on the finite-difference solution is to shift the loading somewhat from the rear to the front of the rotor disk. Accordingly, the greatest trim effect is on the lateral cyclic input (Fig. 9). Furthermore, the effect of the finite-difference solution is to bring the trim settings into somewhat closer accord with the experimental values. Note also that the trim settings are essentially fixed after the first iteration.

At present, the only available pressure data are for the upper blade surface at $r/R = 0.95$. The comparison of the measured and computed upper-surface pressures is shown in Fig. 10. A similar pressure comparison at an advance ratio of 0.345 is shown in Fig. 11. There is a considerable difference between measured and computed pressures in the first quadrant where the pressures appear to be generally underpredicted. The comparison tends to be better in the second quadrant, where the shock location is correctly predicted.

Concluding Remarks

The above results are an indication of the most probable immediate direction of finite-difference computations for application to high-speed rotor loads. The mixed integral-differential approach to transonic load prediction has the advantage of making immediate use of our existing loads codes. It also can greatly reduce the need for two-dimensional airfoil testing. (It should be borne in mind that two-dimensional profile data are probably of dubious value when non-rectangular planforms or transonic unsteadiness are involved.) In its present stage of development, the approach gives fair to good comparison with experimental pressure data. However, considerably more comparisons with forward flight data are required. The method clearly can be enhanced by employing a conservative, full-potential finite-difference model and by improving the near-wake modeling capability. This latter improvement would involve inserting the moving vortex back into the finite-difference grid. Such

modifications will certainly be required if the method is to be extended to lower advance ratios at which the blade/vortex interactions are more important.Even in its present form, however, the mixed integral-differential scheme affords a considerable improvement in our flow prediction capabilities.

In the future, finite-difference modeling can be developed and extended for application to a wider variety of problems, the most important of which is probably the prediction of rotor-wake behavior. Ultimately, it will not be unreasonable to expect the development of unified finite-difference models of the entire rotor/fuselage. However, this goal will require many fundamental advances in numerical modeling and in basic flow physics.

References

[1]Murman, E. M. and Stremel, P. M., "A Vortex Wake Capturing Method for Potential Flow Calculations," AIAA Paper 82-0947, June 1982.

[2]Roberts, T. W. and Murman, E. M., "A Computational Method for Helicopter Vortex Wakes," AIAA Paper 84-1554, June 1984.

[3]Steger, J. L. and Caradonna, F. X., "A Conservative, Implicit Finite-Difference Algorithm for the Unsteady Transonic Full Potential Equations," AIAA Paper 80-1368, July 1980.

[4]Chang, I. C., "Transonic Flow Analysis for Rotors. Part 2, Three-Dimensional, Unsteady, Full-Potential Calculation," NASA TP-2375, 1985.

[5]Caradonna, F. X. and Tung, C., "Experimental and Analytical Studies of a Model Helicopter Rotor in Hover," NASA TM-81232, 1981.

[6]Caradonna, F. X., Desopper, A., and Tung, C., "Finite Difference Modeling of Rotor Flows Including Wake Effects," Journal of the American Helicopter Society, Vol. 29, No. 2, Apr. 1984.

[7]Summa, J. M. and Clark, D. R., "A Lifting-Surface Method for Hover/Climb Loads," Paper 79-1, 35th Annual National Forum of the American Helicopter Society, Washington, D.C., May 1979.

[8]Caradonna, F. X., "The Transonic Flow on a Helicopter Rotor," Ph.D. Dissertation, Stanford University, Stanford, Calif., Mar. 1978.

[9]Chattot, J. J., "Calculation of Three-Dimensional Unsteady Transonic Flows past Helicopter Blades," NASA TP-1721, 1980.

[10]Tung, C., Caradonna, F. X., Boxwell, D. A., and Johnson, W. R., "The Prediction of Transonic Flows on Advancing Rotors," Paper 84-40-44, 40th Annual National Forum of the American Helicopter Society, Arlington, Va., May 1984.

[11]Johnson, W., "A Comprehensive Analytical Model of Rotorcraft Aerodynamics and Dynamics. Part 1, Analysis Development," NASA TM-81182, 1980.

[12]Boxwell, D. A., Schmitz, F. H., Splettstoesser, W. R., and Schultz, K. J., "Model Helicopter Rotor High-Speed Impulsive Noise: Measured Acoustics and Blade Pressures," NASA TM-85850, 1983.

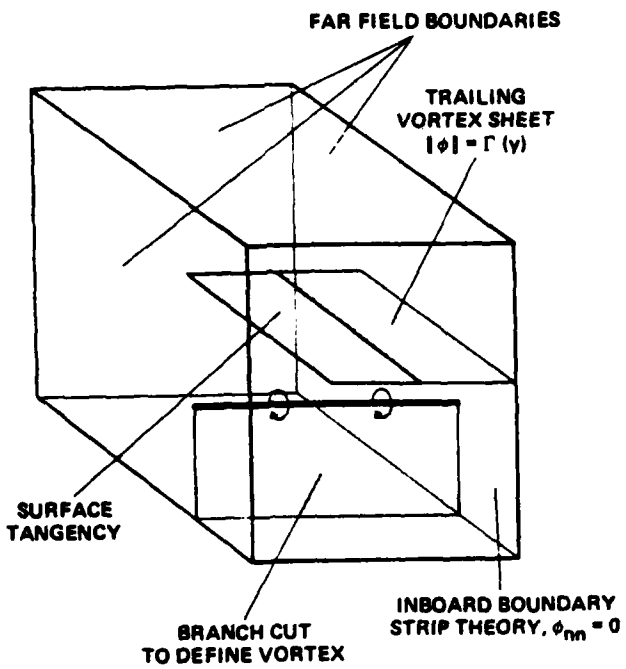

Fig. 1 Boundary conditions for the rotor potential-flow problem.

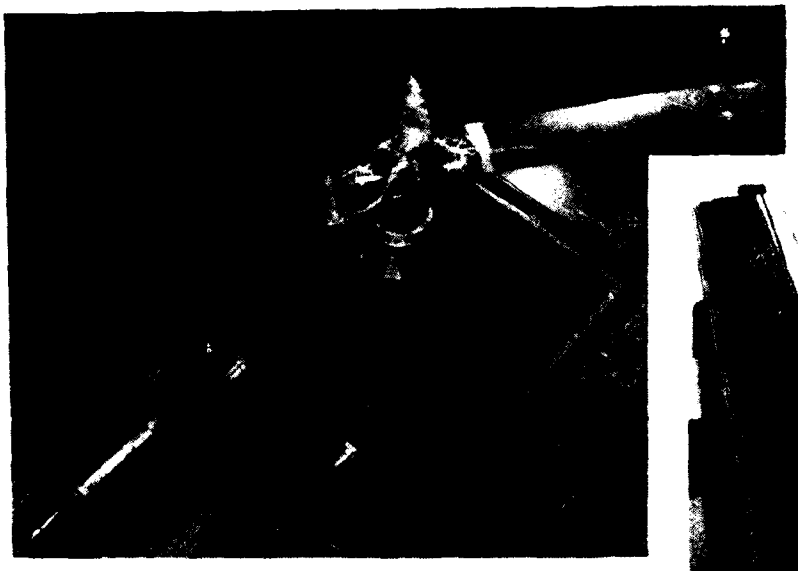

ROTOR BALANCING

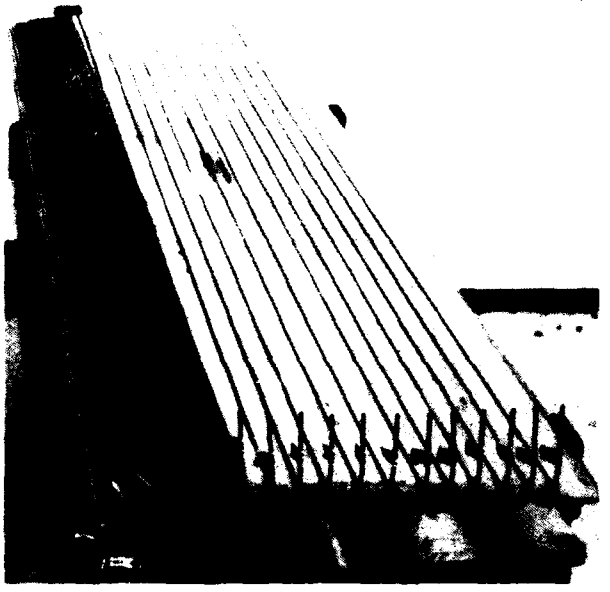

BLADE CONSTRUCTION

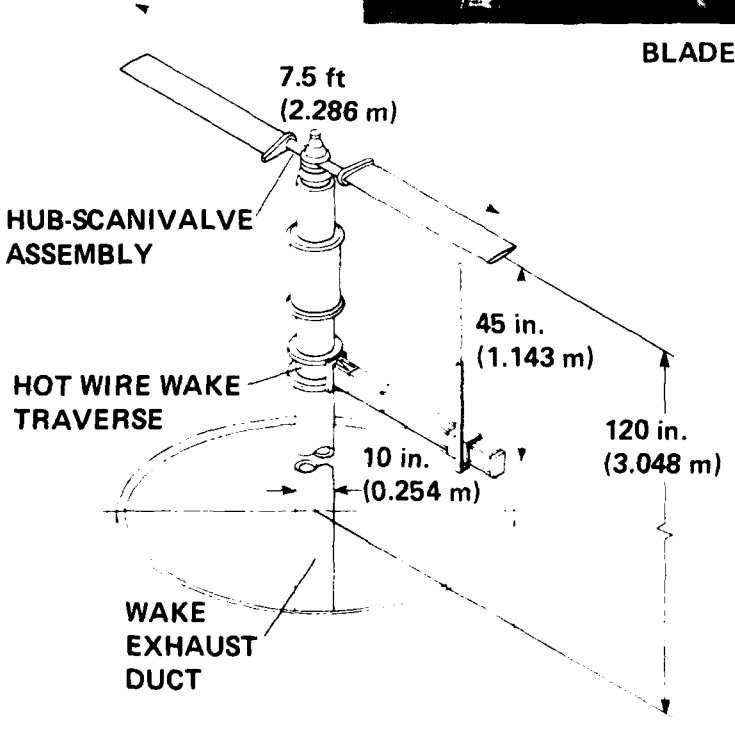

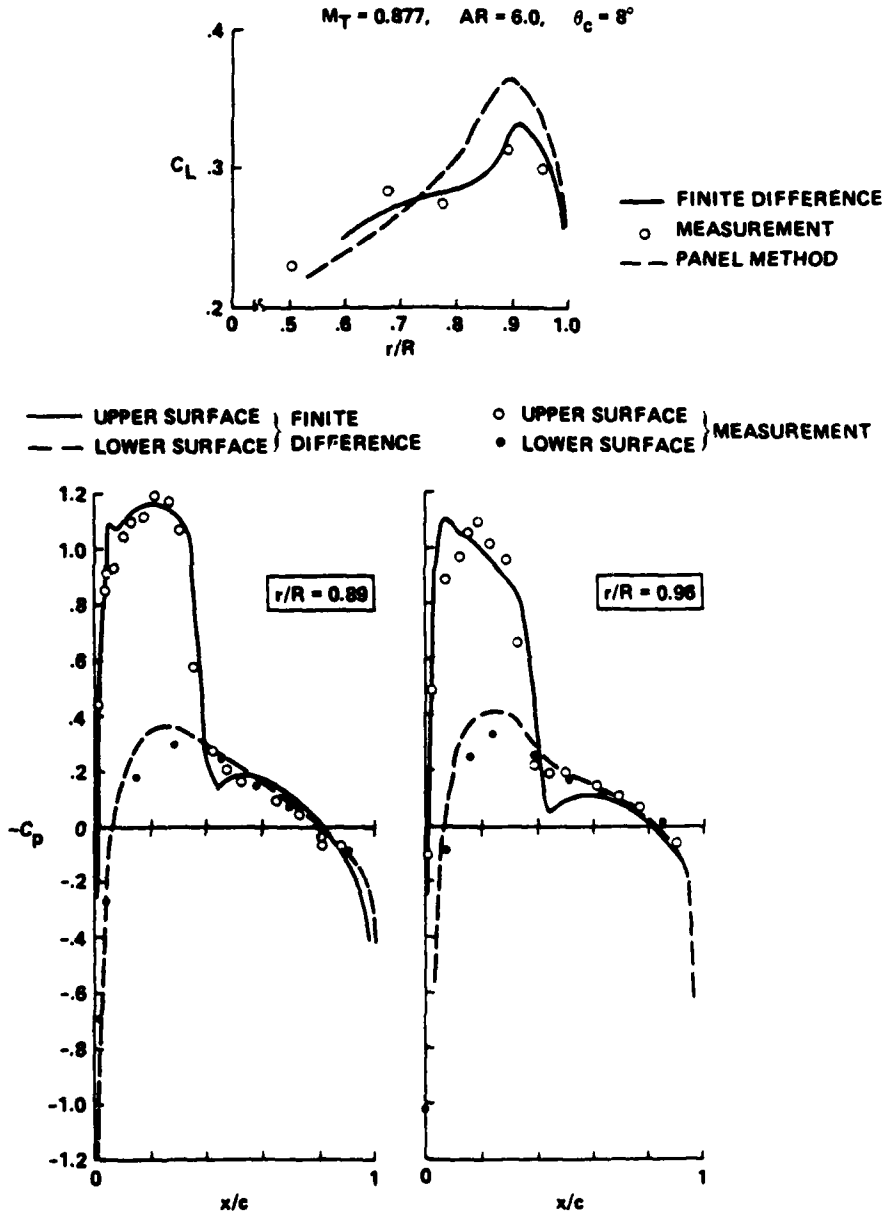

a) r/R = 0.89 and 0.96.

Fig. 3 Comparison of measured and computed chordwise pressure distributions for hover model: M_T = 0.877, AR = 6.0, θ_c = 8°.

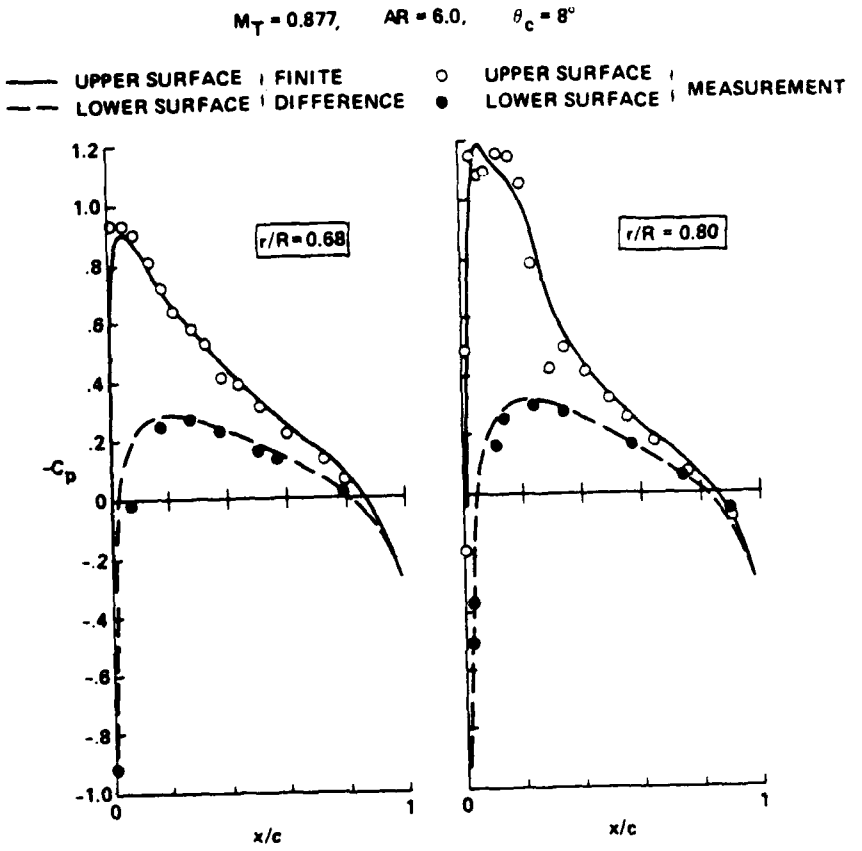

b) r/R = 0.68 and 0.80.

Fig. 3 Concluded.

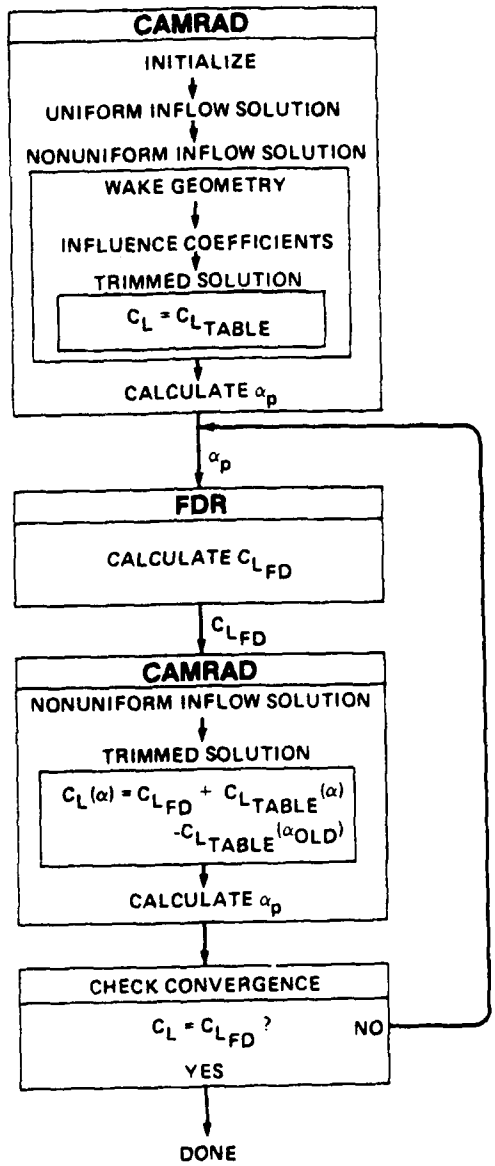

Fig. 4 A hybrid integral-differential rotor flow scheme.

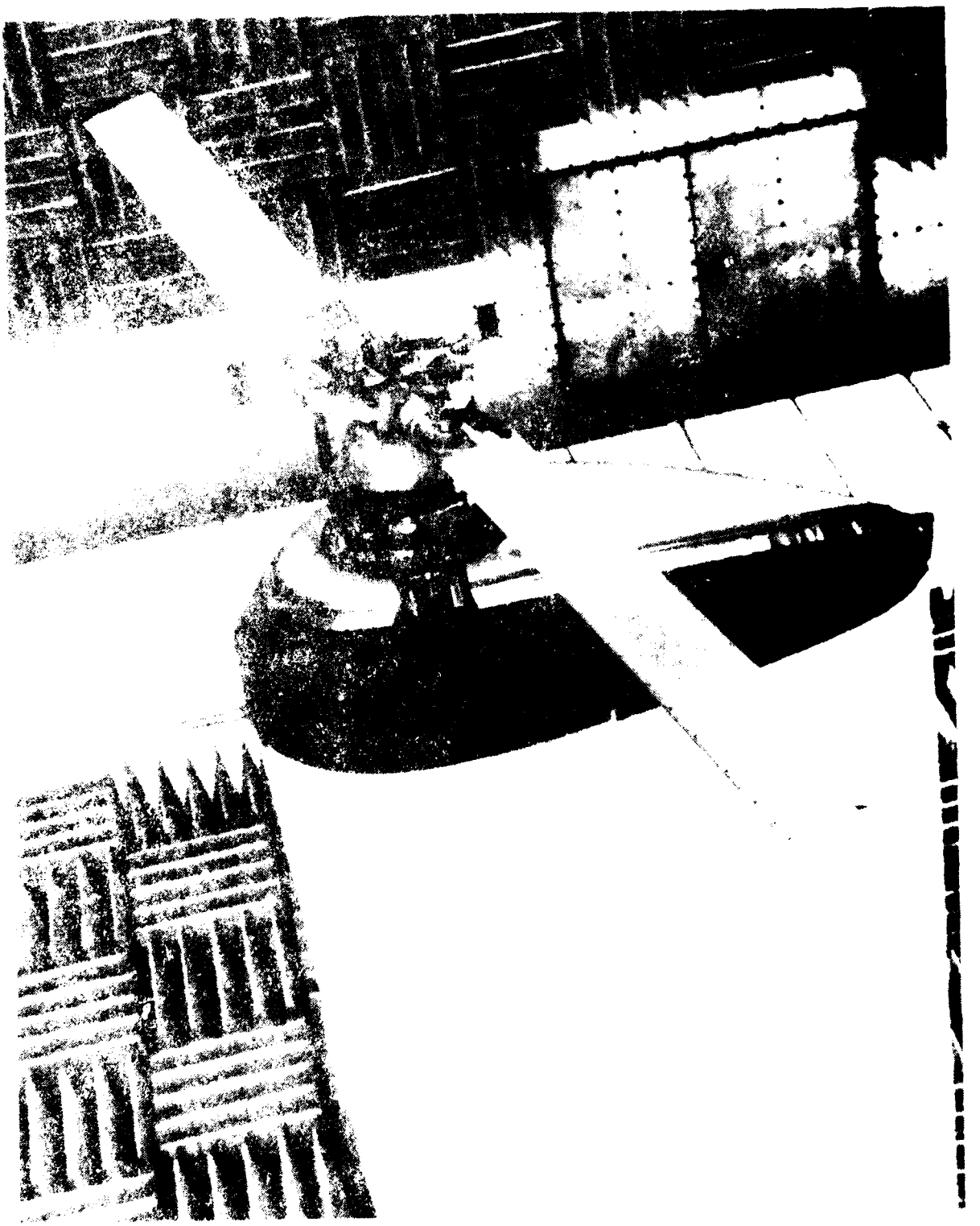

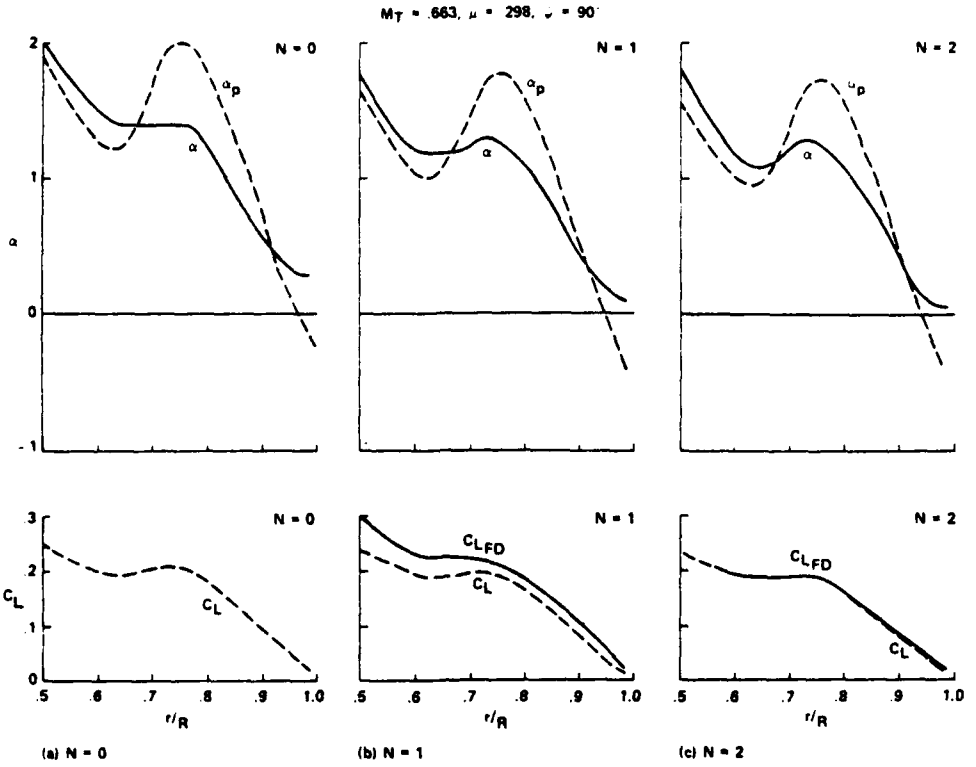

Fig. 6 Evolution of the load and angle-of-attack distribution with CAMRAD-FDR iteration number: M_T = 0.663, μ = 0.298, ψ = 90°.

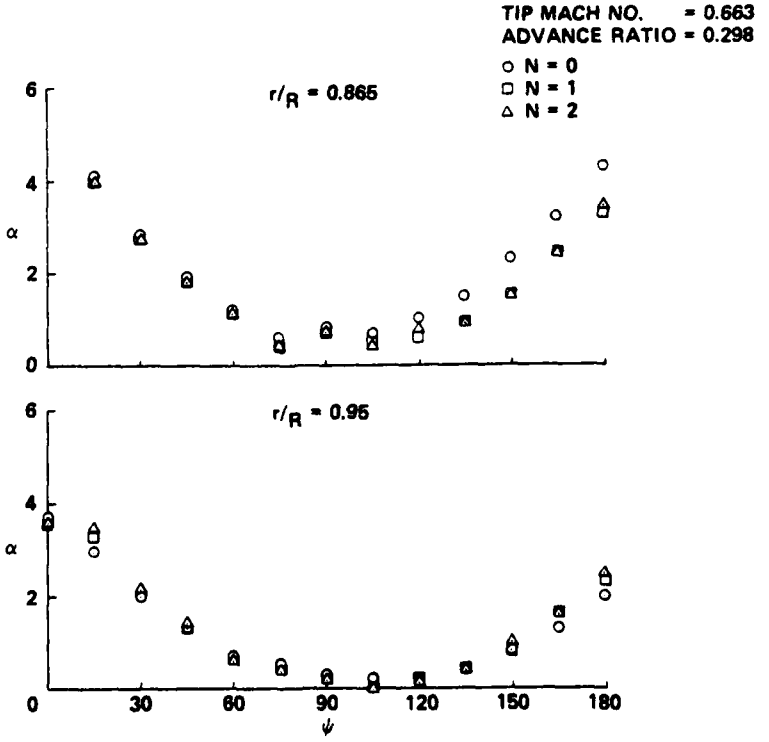

Fig. 7 Azimuthal inflow variation as a function of iteration number: M_T = 0.663, μ = 0.298.

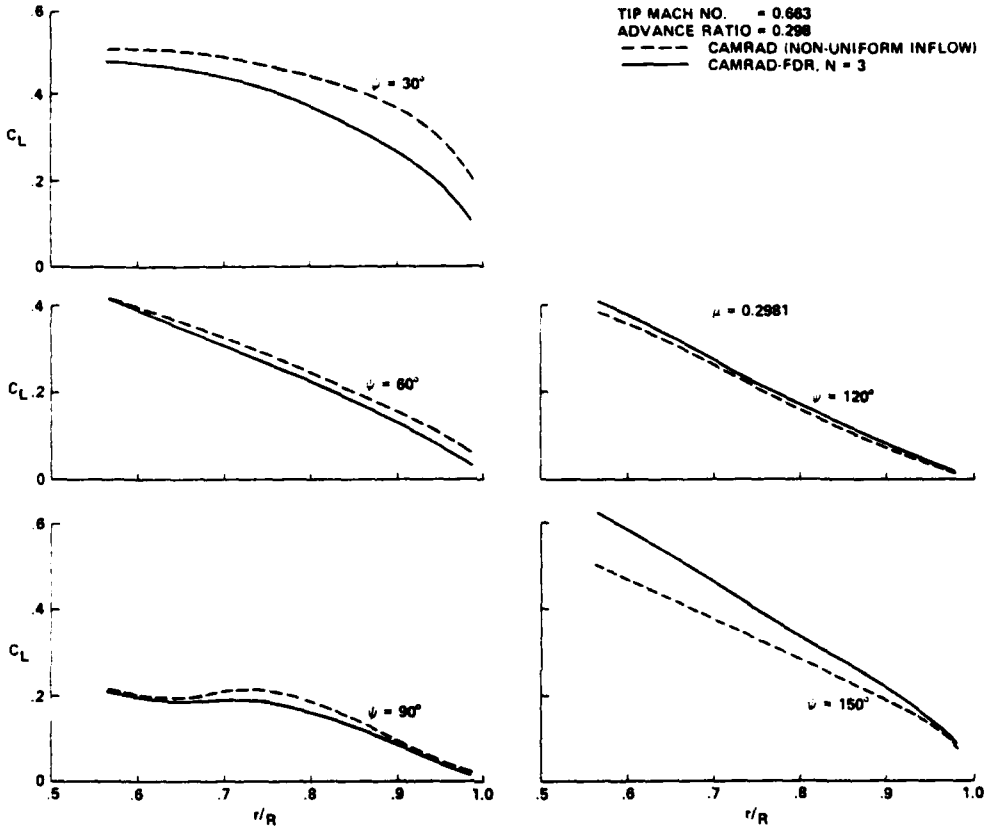

Fig. 8 Radial lift distribution for comprehensive lifting-line and finite-difference computations: $M_T = 0.663$, $\mu = 0.298$.

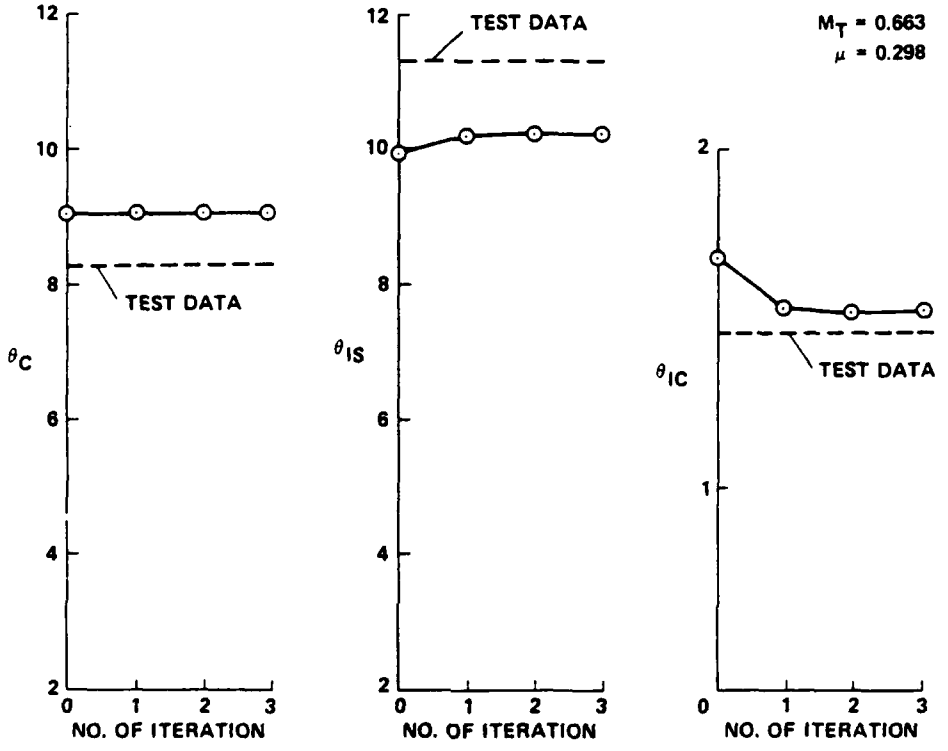

Fig. 9 Effect of CAMRAD-FDR iteration number on trimmed collective and cyclic inputs: M_T = 0.663, μ = 0.298.

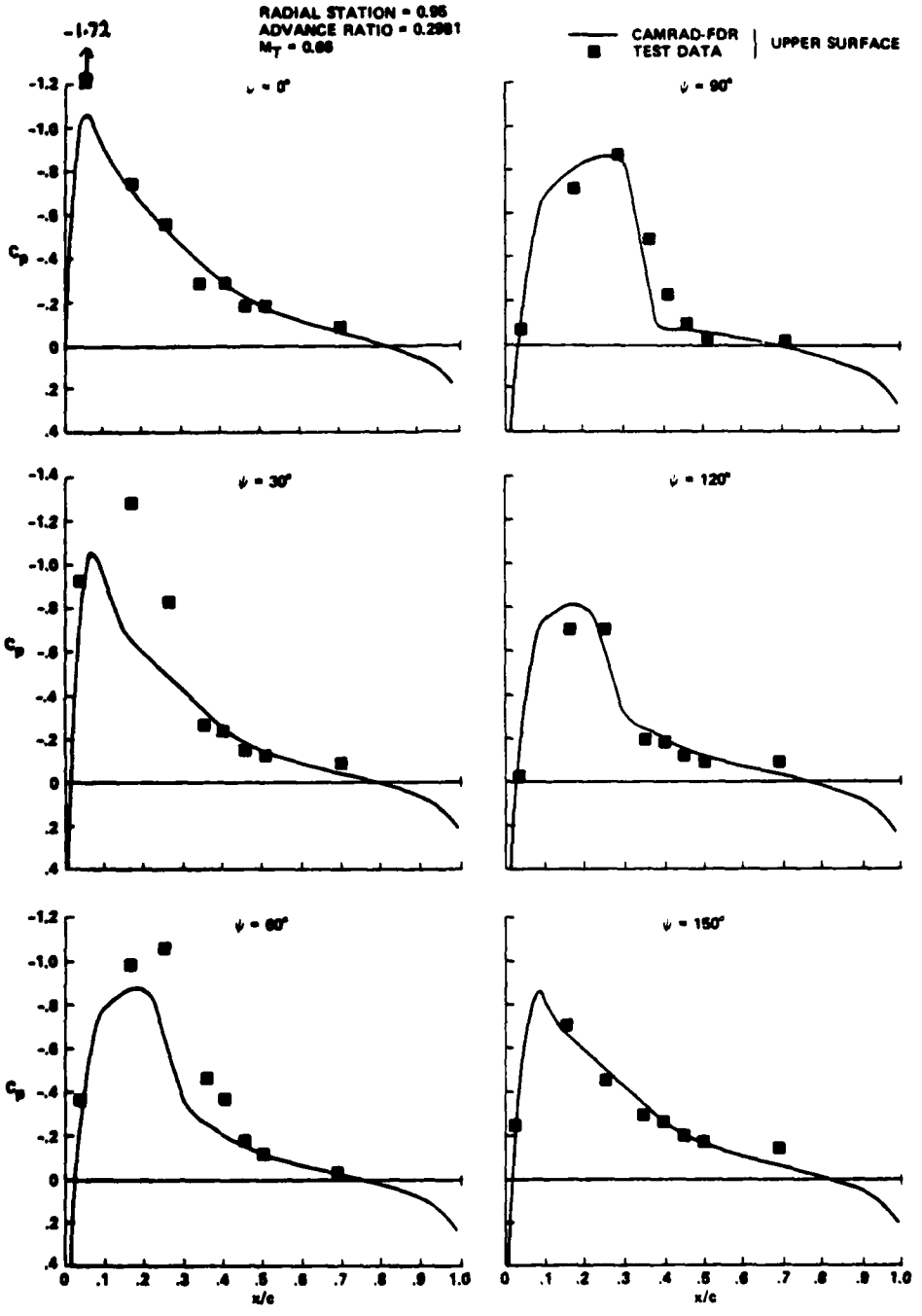

Fig. 10 Comparison of computed and experimental surface pressure for an advancing rotor: M_T = 0.663, μ = 0.298, r/R = 0.95.

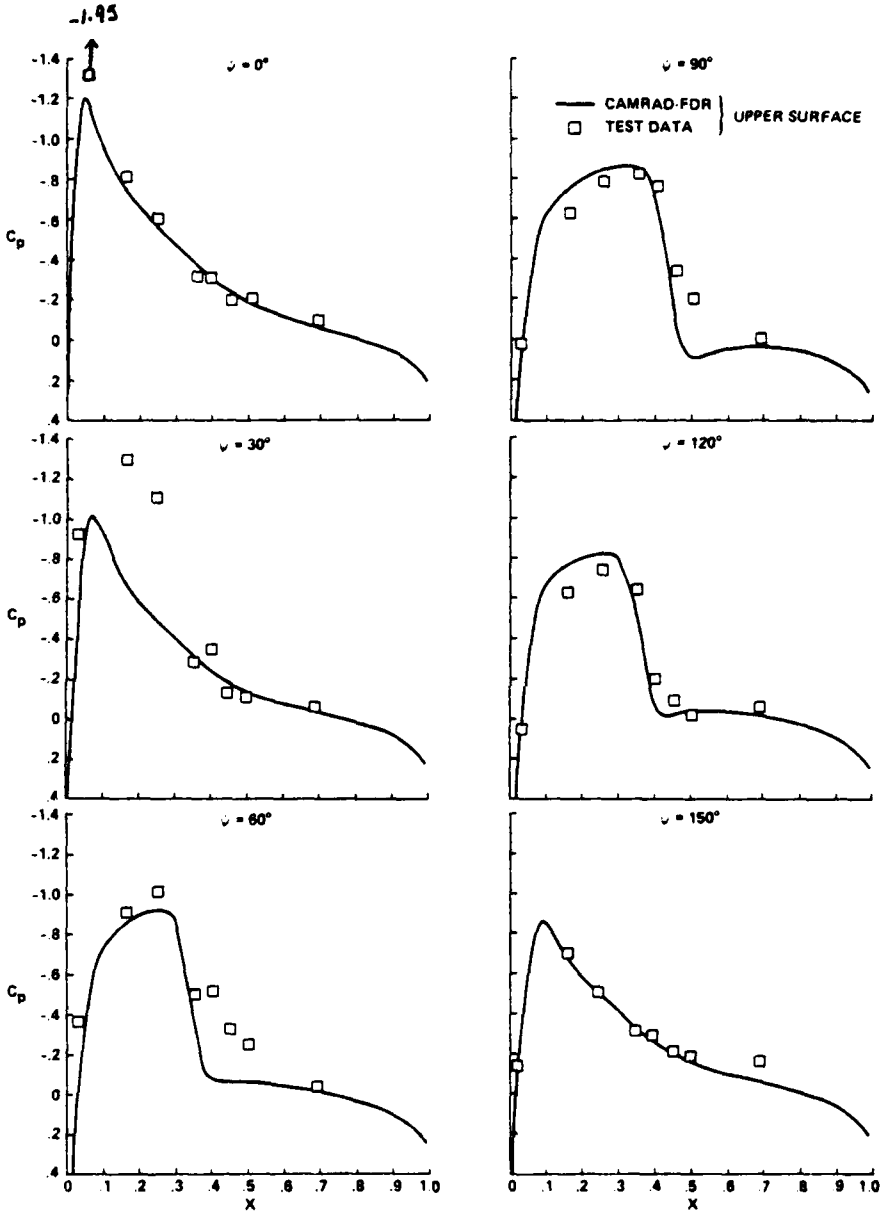

Fig. 11 Comparison of computed and experimental surface pressures for an advancing rotor: $M_T = 0.663$, $\mu = 0.3452$, $r/R = 0.95$.

1. Report No.	2. Government Accession No.	3. Recipient's Catalog No.
NASA TM-86682	AD-A155 581	

4. Title and Subtitle	5. Report Date
FINITE-DIFFERENCE COMPUTATIONS OF ROTOR LOADS	April 1985
	6. Performing Organization Code

7. Author(s)	8. Performing Organization Report No.
F. S. Caradonna and C. Tung	85132
	10. Work Unit No.

9. Performing Organization Name and Address	11. Contract or Grant No.
Aeromechanics Laboratory, U.S. Army Research and Technology Laboratories--AVSCOM NASA Ames Research Center Moffett Field, CA 94035	
	13. Type of Report and Period Covered
12. Sponsoring Agency Name and Address	Technical Memorandum
National Aeronautics and Space Administration Washington, DC 20546	14. Sponsoring Agency Code

15. Supplementary Notes

Point of contact: F. X. Caradonna, Ames Research Center, MS 215-1, Moffett Field, CA 94035. (415) 694-5902 or FTS 464-5902

16. Abstract

This paper demonstrates the current and future potential of finite-difference methods for solving real rotor problems which now rely largely on empiricism. The demonstration consists of a simple means of combining existing finite-difference, integral, and comprehensive loads codes to predict real transonic rotor flows. These computations are performed for hover and high-advance-ratio flight. Comparisons are made with experimental pressure data.

17. Key Words (Suggested by Author(s))	18. Distribution Statement
Rotor Transonics	Unlimited Subject Category - 02

19. Security Classif. (of this report)	20. Security Classif. (of this page)	21. No of Pages	22. Price*
Unclassified	Unclassified	19	A02

*For sale by the National Technical Information Service, Springfield, Virginia 22161

END

FILMED

7-85

DTIC